

# Indentation and Scratch Tests on Sputtered Amorphous $CN_x$ Films Deposited on Plasma-Nitrided Ti-6Al-4V

Yongqing Fu, Nee Lam Loh, Bibo Yan, and Jun Wei

(Submitted 5 October 1999; in revised form 30 May 2000)

Sputtered carbon nitride ( $CN_x$ ) films were deposited on both untreated and plasma-nitrided Ti-6Al-4V substrates. Surface and cross-section morphology of the deposited  $CN_x$  films was studied by scanning electron microscopy (SEM). Modified Vickers hardness tests showed that the intrinsic hardness of the  $CN_x$  film was about HV 2000 to 3000. Both the indentation and scratch tests showed that, compared with the  $CN_x$  film deposited on Ti-6Al-4V substrate, the load-bearing capacity of  $CN_x$  film deposited on a plasma-nitrided layer was improved dramatically. From the results of scratch tests, the duplex-treated system was effective in maintaining a favorable low and stable coefficient of friction and improving the wear resistance of Ti-6Al-4V substrate.

**Keywords** carbon nitride, duplex treatment, indentation, scratch test, Ti-6Al-4V, wear

## 1. Introduction

Based on theoretical calculations, Liu and Cohen<sup>[1]</sup> predicted a metastable binary phase of carbon and nitrogen, namely,  $\beta-C_3N_4$ , with bulk modulus equal to or greater than that of diamond.<sup>[2]</sup> This remarkable prediction stimulated intense theoretical and experimental activity worldwide with a view to synthesize this superhard material.<sup>[3,4,5]</sup> However, up to now, even though a variety of deposition techniques have been used to prepare carbon nitride films, the deposits were usually amorphous (sometimes, with small clusters of microcrystalline material<sup>[6,7]</sup>) and mostly substoichiometric in nitrogen, *i.e.*, the formation of amorphous carbon nitride films ( $CN_x$ ), with  $X$  typically about 0.3 to 0.5.<sup>[4]</sup> Amorphous  $CN_x$  films have already been applied in the magnetic recording industry rivalling the amorphous diamond-like carbon (DLC) films with their high hardness and elastic property, superior heat conductivity, and low friction coefficient.<sup>[8]</sup> Amorphous carbon nitride films have also been prepared on Ti alloys for improving their tribological properties and biocompatibility.<sup>[9,10]</sup> However, the soft Ti alloys may not be able to provide adequate support for the hard  $CN_x$  films, thereby adversely affecting their load-bearing capacity, tribological performance, and durability. An approach to solve this problem is to design and develop duplex diffusion/coating treatments.<sup>[11,12]</sup>

Duplex surface engineering involves the sequential application of two (or more) established surface technologies to produce a surface composite with combined properties that are unobtainable through any individual surface technology.<sup>[13]</sup> Current studies on duplex treatments concentrate on combining

plasma nitriding with TiN, CrN, or DLC coating on steel substrate.<sup>[14,15,16]</sup> However, so far, there are no reports on the duplex-treatment combining of plasma nitriding with  $CN_x$  films on Ti alloy substrate. The purpose of this research work is to study the combination of plasma nitriding and  $CN_x$  films on Ti-6Al-4V substrate.

The best tribological coating should combine high hardness, low coefficient of friction, and high load-bearing capacity (not only the high adhesion strength).<sup>[17]</sup> To measure the load-bearing capacity and mechanical properties of thin films, it is required that the strains be introduced in a systematic manner. For a relatively brittle film on a ductile substrate, this can be achieved by transferring strains through deforming the substrate, *i.e.*, by indentation or impression.<sup>[18,19]</sup> In this study, the Rockwell indentation tests were performed on  $CN_x$  films deposited on both untreated and plasma-nitrided Ti-6Al-4V to compare their static load-bearing capacity.<sup>[13,17]</sup>

Higher coating hardness and lower coefficient of friction are desirable for good tribological performances of  $CN_x$  films. However, high hardness usually corresponds with brittleness and high stress in the coating, which may degrade both the load-bearing capacity and the tribological performance.<sup>[20]</sup> In this study, a scratch test machine was used to evaluate both the dynamic load-bearing capacity<sup>[13]</sup> and tribological behavior of  $CN_x$  coating deposited on untreated and plasma-nitrided Ti-6Al-4V.

## 2. Experimental Details

Ti-6Al-4V plates with a diameter of 50 mm and a thickness of 3 mm were ground with SiC grinding papers and polished with diamond pastes, then ultrasonically rinsed in acetone. Plasma nitriding was carried out with a total power of 2 kW and a voltage of 1500 V. The deposition temperature was 800 °C and the nitriding duration was 9 h.  $CN_x$  films were deposited on untreated and plasma-nitrided Ti-6Al-4V plates by an unbalanced magnetron sputtering system under a base pressure of  $6 \times 10^{-3}$  Pa. A high purity (99.99%) planar graphite target was used in a pure (99.999%) nitrogen discharge at a gas

Yongqing Fu, Nee Lam Loh, and Bibo Yan, Materials Laboratory, School of Mechanical and Production Engineering, Nanyang Technological University, Singapore, 639798; and Jun Wei, GINTIC Institute of Manufacturing Technology, Singapore, 638075. Contact e-mail: myqfu@ntu.edu.sg.

pressure of 5 Pa and a constant gas flow rate of 40 standard-cubic-centimeter-per-minute. The discharge current on the cathode was held at 1 A, the substrate temperature was below 200 °C, and the negative substrate bias voltage was −300 V.

The surface and cross-section morphology of the duplex-treated system and the deposited  $CN_x$  films was investigated by a JEOL (Japan Electron Optics Ltd., Tokyo) scanning electron microscope (SEM). Transmission electron microscopy, Fourier transform infrared spectroscopy, Raman spectroscopy, and x-ray photoelectron spectroscopy (XPS) analysis of  $CN_x$  films can be found in Ref 12.

The intrinsic hardness was evaluated using Vickers microhardness tests proposed by Jonsson and Hogmark:<sup>[21,22]</sup>

$$H_f = H_s + \frac{K_c - K_s}{2 \times C \times t} \quad (\text{Eq 1})$$

where  $H_f$  is the intrinsic film hardness and  $H_s$  is substrate hardness. The terms  $K_c$  and  $K_s$  are the slopes of the curves of measured hardness versus reciprocal of the indentation diagonal for the coated sample and substrate, respectively;  $C$  is the constant factor determined by indentation geometry; and  $t$  is the film thickness. However, one of the problems for this equation is the choice of the  $C$  value for different film-substrate systems. Xu *et al.*<sup>[23,24]</sup> modified the parameters according to different hardness ratios and found the intrinsic hardness to be Eq 2:

$$H_f = H_s \times \left[ \frac{A - 1}{2} + \sqrt{\left( \frac{A - 1}{2} \right)^2 + A + 2} \right] \quad (\text{Eq 2})$$

where  $A = (K_c - K_s)/(t \times H_s)$ . In this research work,  $CN_x$  thin films with thicknesses of 2 and 5  $\mu\text{m}$  were deposited on both Ti-6Al-4V and plasma-nitrided Ti-6Al-4V. A MICROMET II microhardness tester was used and the loads for Vickers hardness ranged from 50 g to 10 kg, respectively. The calculated procedures were previously described.<sup>[21–25]</sup>

The load-bearing capacity of the duplex-treated Ti-6Al-4V was evaluated using a Rockwell hardness tester under the normal loads of 588 and 1470 N. With the Rockwell hardness tester (Matsuzawa Seiki Co. Ltd., Tokyo, Japan), static load-bearing capacity of a film was judged from the radial and lateral cracks and spallation after the indentation using an SEM. Tribological performance and dynamic load-bearing capacity of the  $CN_x$  films on different substrates were assessed using a scratch tester.<sup>[26,27]</sup> A diamond stylus was driven across the coating to determine the load-bearing capacity at a constant speed of 1 mm/s and a continuously increased load rate of 1.5 N/s. Determination of the critical load for coating failure, which is related to the load-bearing capacity of a coating-substrate system, was made by metallurgical examination of the scratch traces. During the scratch test, both the tangential force and normal loads were measured continuously, and the coefficient of friction can be obtained from the ratio of the tangential force to normal load. By comparing the curves of coefficient of friction versus normal load for four types of specimens (*i.e.*, Ti-6Al-4V, plasma-nitrided Ti-6Al-4V, and  $CN_x$  films deposited on both untreated and plasma-nitrided Ti-6Al-4V), their tribological behavior can be evaluated.

### 3. Results and Discussion

#### 3.1 Characterization of $CN_x$ and Duplex-Treated Coating

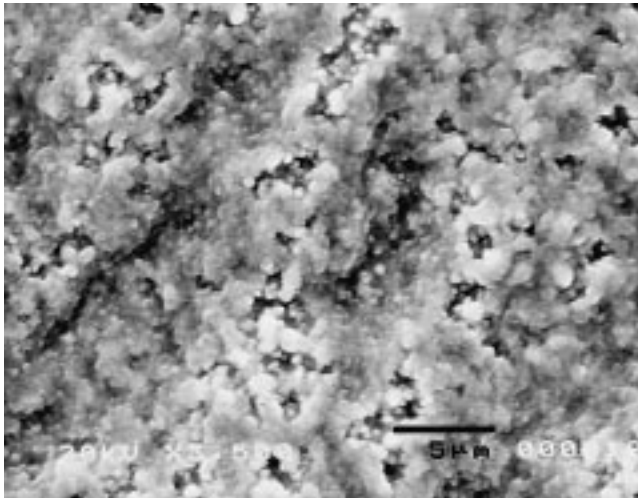
Physically,  $CN_x$  films are opaque, dark-brown in color, smooth, with good adherence to the substrate, and appear to replicate the substrate topography. Figure 1(a) to (c) show the SEM surface morphology of plasma-nitrided Ti alloys (800 °C, 9 h) and carbon nitride films deposited on both Ti-6Al-4V substrate and plasma-nitrided specimen. The plasma-nitrided surface is very rough, which is typical for the surface after plasma ion bombardment and irregular growth of nitride, as shown in Fig. 1(a). The surface of  $CN_x$  films deposited on a Ti-6Al-4V substrate is relatively smooth, as shown in Fig. 1(b). The SEM observation indicates that the deposition of  $CN_x$  film has a smoothing effect on the plasma-nitrided layer, as shown in Fig. 1(c).

Figure 2 shows the cross-section morphology of the duplex-treated coating system. The  $CN_x$  film with a thickness of 5  $\mu\text{m}$  is dense and free of porosity. Examination at high magnifications reveals a uniform microstructure of  $CN_x$  films at the microlevel. There is no sign of cracking or debonding and continuity is evident across the interfaces among the Ti alloy substrate, nitrided layer, and  $CN_x$  film, indicating good adhesion between the  $CN_x$  film and plasma-nitrided Ti alloy substrate. Beneath the  $CN_x$  film is the plasma-nitrided layer, which is composed of two sublayers. The top sublayer (or the compound layer) consists of  $\delta$ -TiN and  $\epsilon$ -Ti<sub>2</sub>N (up to about 1 to 2  $\mu\text{m}$  thick), as reported in Ref 10 and 12. The lower sublayer between the compound layer and the substrate material contains a nitrogen-rich  $\alpha$ -stabilized solid-solution-hardened zone. The core material consists of retained  $\beta$  phase in a matrix of  $\alpha$ -Ti. The ratio of N/C in the films obtained from XPS is about 0.45, which is far below the desired value of  $\beta$ -C<sub>3</sub>N<sub>4</sub> (1.33).

The regression analysis results of Vickers hardness tests and the calculated coating intrinsic hardness values are listed in Table 1. The calculated results according to Eq 2 show that the intrinsic hardness of  $CN_x$  thin film is about HV 2000 to 3000 (or 20 to 30 GPa) depending on different coating systems, which is about 7 to 9 times higher than that of the Ti-6Al-4V substrate. It seems that with an increase in film thickness, the intrinsic coating hardness decreases. The  $CN_x$  film deposited on a plasma-nitrided layer is a little harder than that deposited on Ti-6Al-4V substrate. However, the reasons are not clear and these conclusions need further investigation.

#### 3.2 Static Load-Bearing Capacity Evaluated by Indentation Tests

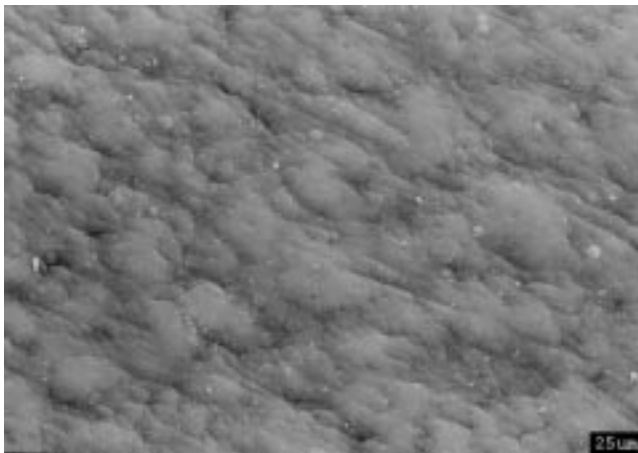
Figure 3 shows the SEM micrographs of the indentation impressions of  $CN_x$  films deposited on Ti-6Al-4V and plasma-nitrided Ti-6Al-4V. For the  $CN_x$  films deposited directly on Ti-6Al-4V substrate, there is usually large-area cracking and spallation occurring after indentation, as shown in Fig. 3(a) and (d). Under a small normal load of 588 N, for a 2  $\mu\text{m}$   $CN_x$  film deposited on plasma-nitrided Ti-6Al-4V substrate, there are some small ring cracks within the impression and ejecting radial cracks formed at the circumference of the indentation, as shown in Fig. 3(e). Under a high normal load of 1470 N, severe radial and ring cracks (but no spallation) can be observed on  $CN_x$



(a)



(b)



(c)

**Fig. 1** SEM surface morphologies of (a) plasma-nitrided Ti alloys (800 °C, 9 h); (b) carbon nitride film deposited on Ti-6Al-4V substrate; and (c) carbon nitride film deposited on plasma-nitrided Ti-6Al-4V

films deposited on plasma-nitrided substrates, as shown in Fig. 3(f). With the increase of film thickness to 5 μm, there are some large radial cracks accompanied by blister formation and

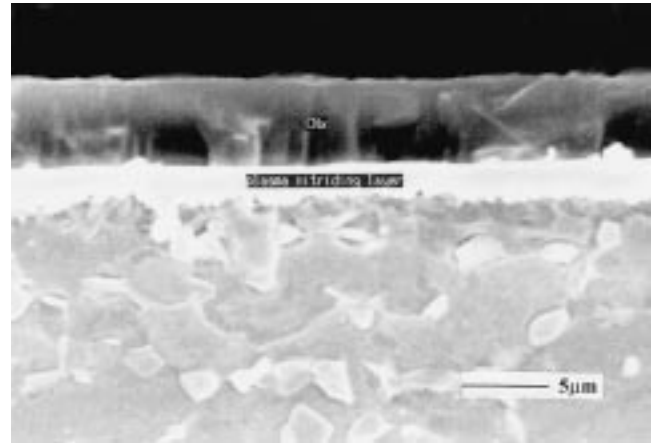


**Fig. 2** The cross-section morphology of the duplex-treated coating system

**Table 1** Regression data for Vickers hardness measurements (CN<sub>x</sub>/PN/Ti64: CN<sub>x</sub> film deposited on plasma-nitrided Ti-6Al-4V; and CN<sub>x</sub>/Ti64: CN<sub>x</sub> film deposited directly on Ti-6Al-4V)

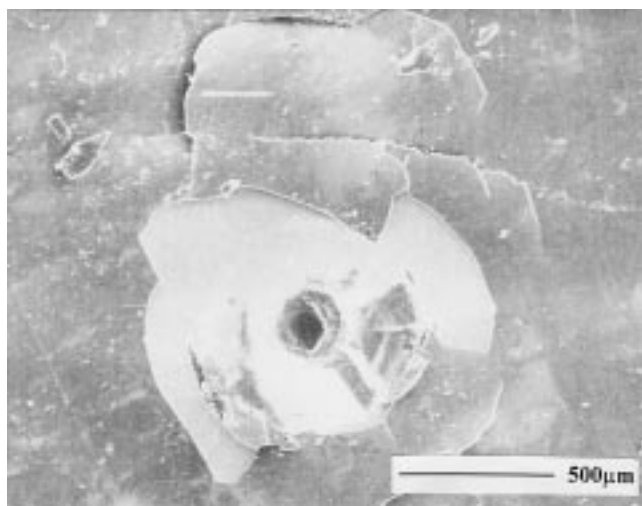
Sample	Thickness of CN <sub>x</sub> films	H <sub>s</sub> (HV or 10 MPa)	K <sub>s</sub> (10 kN/m)	K <sub>c</sub> (10 kN/m)	H <sub>f</sub> (HV or 10 MPa)
CN <sub>x</sub> /PN/Ti64	5 μm	337.13	0.9085	12.583	2576.5
CN <sub>x</sub> /PN/Ti64	2 μm	337.13	0.9085	6.7074	2947.9
CN <sub>x</sub> /Ti64	5 μm	337.13	0.9085	11.939	2292.5

slight debonding of CN<sub>x</sub> films at the edge of the impression, as shown in Fig. 3(g) and (h).

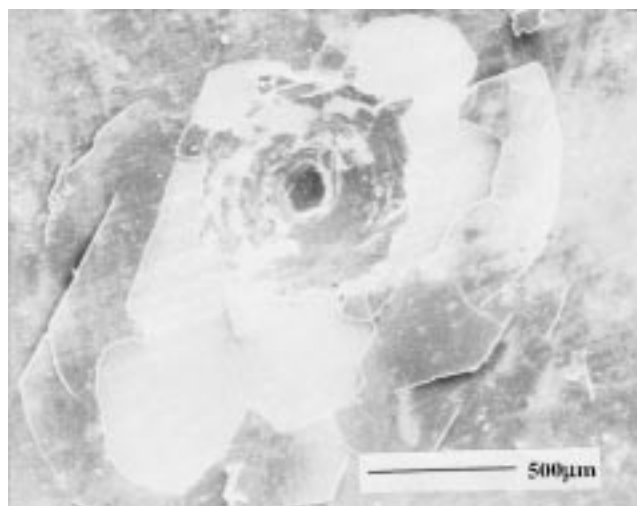
The above results indicate that (1) with the application of a plasma-nitrided interlayer between the substrate and coating, the load-bearing capacity has been improved significantly; and (2) the thicker the films, the poorer the load-bearing capacity. The indentation failure modes of CN<sub>x</sub> films are briefly illustrated in Fig. 4. Figure 4(a) demonstrates a failure mode with only ring cracks and radial cracks around the indentation, which indicate that the coating is brittle but with a high load-bearing capacity.<sup>[16,17]</sup> Figure 4(b) shows that during indentation, many cracks, which form in the coating, reorient along the interface, resulting in discrete debonding, but most of the film remains attached to the substrate.<sup>[28]</sup> This situation corresponds to a film with a relatively poor load-bearing capacity. When there are high stresses in the film due to the sharp difference in elastic modulus or hardness between coating and substrates, the compressed films may buckle at the interface, and these buckles are susceptible to propagation by interface crack growth, followed by large-area spallation, as shown in Fig. 4(c).

### 3.3 Dynamic Load-Bearing Capacity and Tribological Behavior Evaluated by Scratch Tests

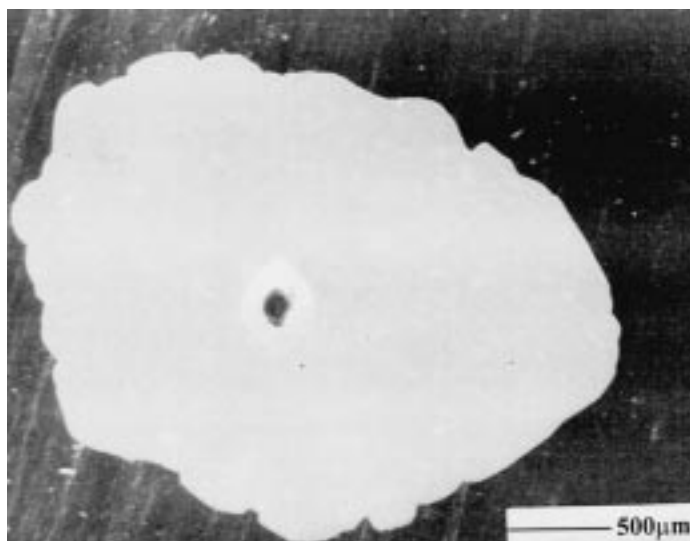
For the scratch tests on CN<sub>x</sub> films, the load-friction curves of coated samples often show a linear increase at the beginning



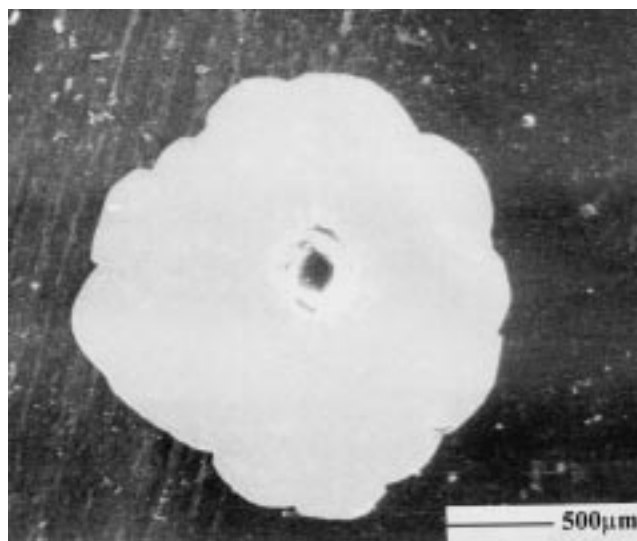
(a)



(b)



(c)



(d)

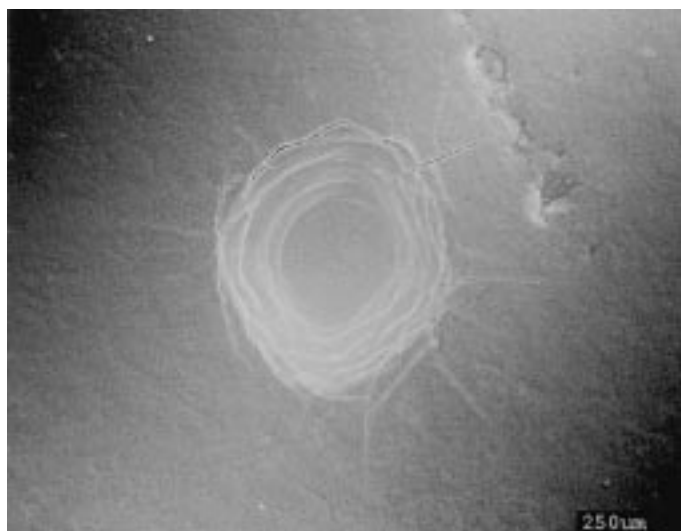
**Fig. 3** The SEM micrographs of the indentation impressions of  $CN_x$  films deposited on Ti-6Al-4V and plasma-nitrided Ti-6Al-4V substrate. (a)  $2\ \mu\text{m}$   $CN_x$ /Ti64 under 588 N; (b)  $2\ \mu\text{m}$   $CN_x$ /Ti64 under 1470 N; (c)  $5\ \mu\text{m}$   $CN_x$ /Ti64 under 588 N; (d)  $5\ \mu\text{m}$   $CN_x$ /Ti64 under 1470 N (continued on next page)

period, with an abrupt increase at a critical load. The critical loads, *i.e.*, the load-bearing capacity of  $CN_x$  films on untreated and plasma-nitrided Ti-6Al-4V substrate, are shown in Fig. 5. Compared with that of carbon nitride film deposited directly on Ti-6Al-4V substrate, the load-bearing capacity is improved dramatically with the application of a plasma-nitrided layer between the Ti-6Al-4V substrate and the  $CN_x$  film. With the increase of thickness of the  $CN_x$  film, the load-bearing capacity becomes poor, probably due to high residual stresses existing in the coating. These results are identical with those from indentation tests.

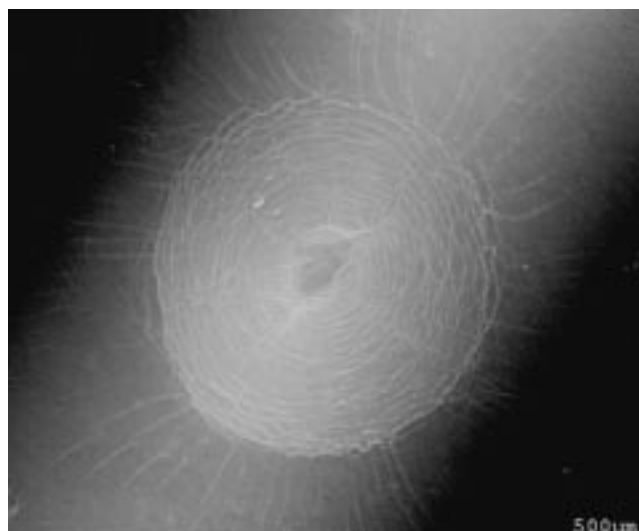
Figure 6 shows the curves of the coefficient of friction versus normal load for different specimens obtained from the friction-load curves of scratch tests. For the stylus scratching on Ti-6Al-4V substrate, the coefficient of friction is about 0.6 to 0.8,

as shown in Fig. 6. Examination of the scratch track shown in Fig. 7 reveals the typical severe abrasive wear (*i.e.*, ploughing). With the stylus scratching on the plasma-nitrided Ti-6Al-4V substrate, the coefficient of friction is low and stable (around 0.15), as shown in Fig. 6. Examination of the wear track shows that there are only slight scratching lines on the wear track, indicating a good wear resistance, as shown in Fig. 8. When the load is increased to about 55 N, there is a large variation in coefficient of friction, which is probably caused by the collapse of the nitrided layer under high normal load.

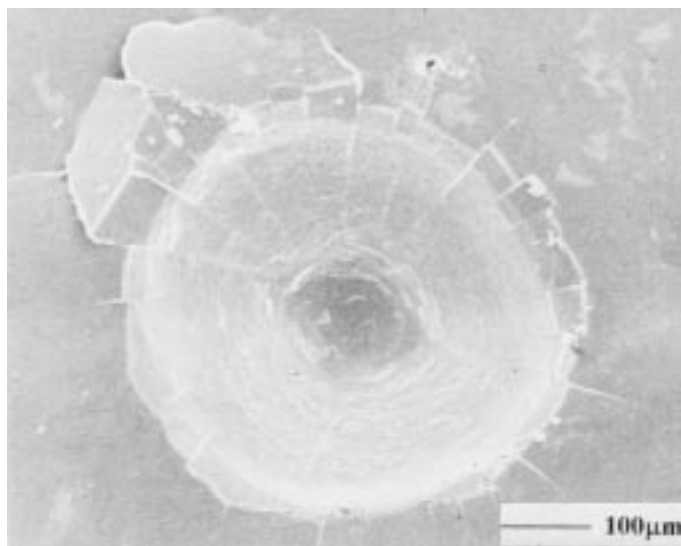
For the scratch test of  $CN_x$  film deposited on Ti-6Al-4V substrate, during the beginning period, the coefficient of friction is very low, as shown in Fig. 6, indicating a good lubricating effect of  $CN_x$  films. However, after a short period, the coefficient of friction increases abruptly. The SEM observation, as



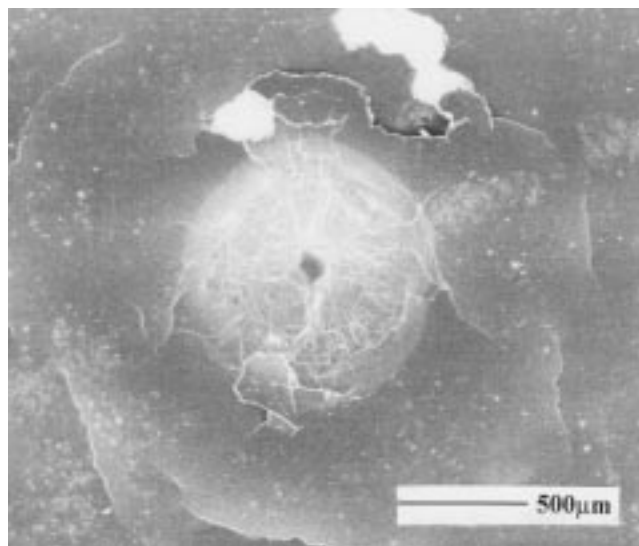
(e)



(f)



(g)



(h)

**Fig. 3 cont.** The SEM micrographs of the indentation impressions of  $CN_x$  films deposited on Ti-6Al-4V and plasma-nitrided Ti-6Al-4V substrate. (e)  $2 \mu m$   $CN_x/PN/Ti64$  under 588 N; (f)  $2 \mu m$   $CN_x/PN/Ti64$  under 1470 N; (g)  $5 \mu m$   $CN_x/PN/Ti64$  under 588 N; and (h)  $5 \mu m$   $CN_x/PN/Ti64$  under 1470 N

shown in Fig. 9, reveals that this sudden increase in friction force is attributed to the spallation of  $CN_x$  film.

For the  $2 \mu m$   $CN_x$  film deposited on prenitrided specimen, the long-term coefficient of friction is shown in Fig. 6. The typical scratch morphology on a duplex-treated surface indicated a mild wear on  $CN_x$  film. There is a sudden jump in friction force occurring at a critical load around 60 N, as shown in Fig. 6. The SEM examination reveals that the film cannot endure the combination of the high normal load and frictional force, so it collapses and causes the large-area spallation of the film, as shown in Fig. 10. A similar phenomenon can be observed for the  $5 \mu m$   $CN_x$  films deposited on a plasma-nitrided surface, and the only difference is that the long-term coefficient of friction is a little lower and the critical load is slightly smaller.

The relatively low coefficient of friction under a higher normal load is probably related to the graphitization of  $CN_x$  coating under high load and sliding conditions,<sup>[29]</sup> but this needs further investigation.

Plasma nitriding of Ti-6Al-4V produces a graded hardened case that can serve as a supporting layer for the hard  $CN_x$  films, improving load-bearing capacity, and it also provides a compressive stress that can assist in excellent fatigue resistance and impart better stability of carbon nitride films to the Ti substrate. Hard and low-friction  $CN_x$  films could effectively reduce the coefficient of friction, thus providing a good tribological behavior. After plasma nitriding, usually the surface becomes rough and the high surface roughness gives a highly stressed layer. By depositing  $CN_x$  films on the plasma-nitrided

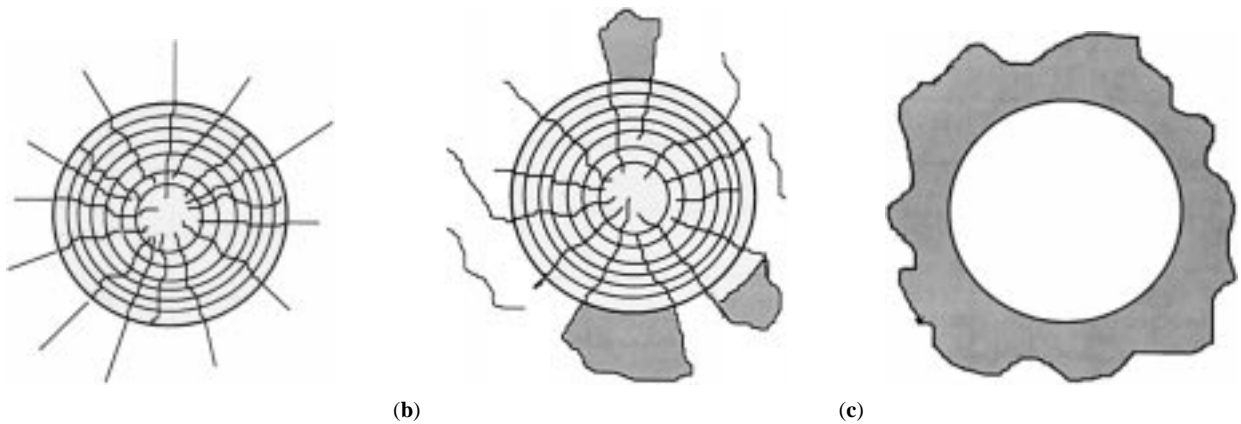


**Fig. 4** The indentation failure modes for  $CN_x$  films deposited on different substrates (a) good load-bearing capacity, (b) poor load-bearing capacity, and (c) poor load-bearing capacity

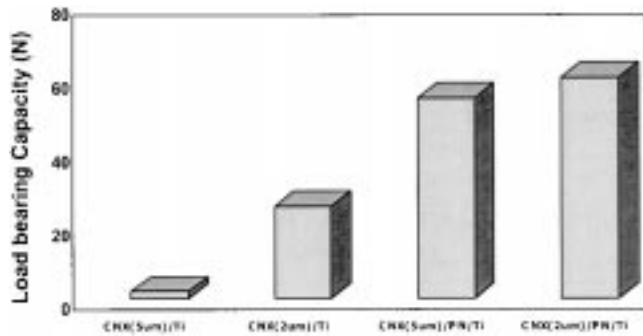


**Fig. 5** The load-bearing capacity of  $CN_x$  films on untreated and plasma-nitrided Ti-6Al-4V substrate obtained from the scratch tests

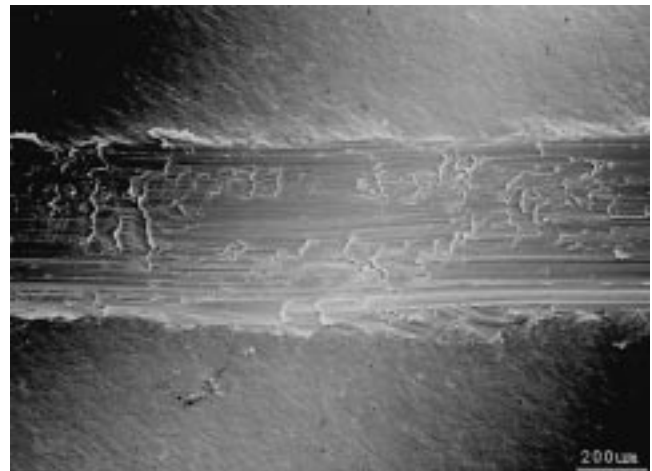


**Fig. 7** The typical severe abrasive wear (*i.e.*, ploughing) observed on the scratch track of Ti-6Al-4V at a normal load range between 30 and 40 N

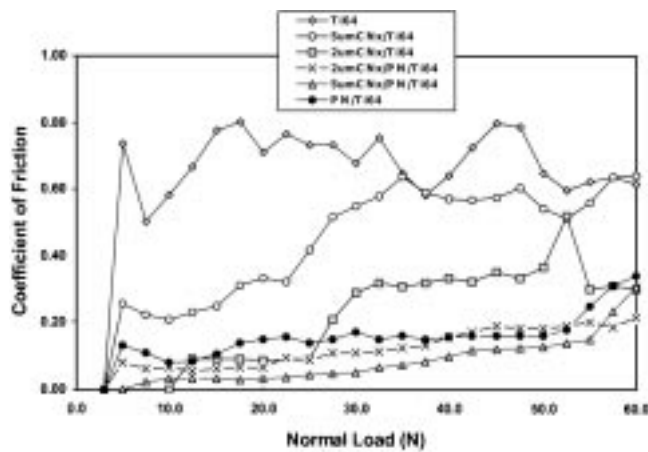


**Fig. 6** The coefficient of friction with increase of normal load for Ti-6Al-4V substrate, plasma-nitrided layer, and  $CN_x$  film deposited on Ti-6Al-4V and on prenitrided layer

specimen, the surface roughness can be decreased; therefore, reinforcing the plasma-nitrided layer by deposition of  $CN_x$  films can improve the wear resistance significantly.<sup>[12,30]</sup>

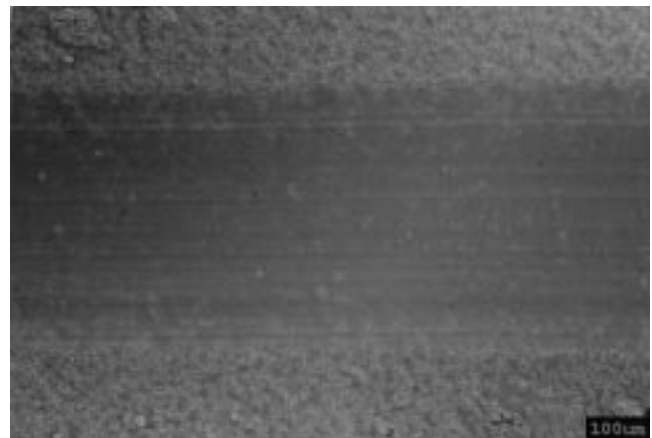


**Fig. 8** The typical morphology of the scratch track on plasma-nitrided surface at a normal load range between 30 and 40 N

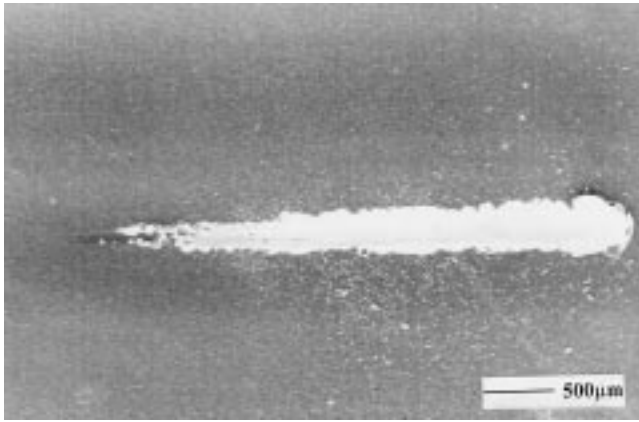


**Fig. 9** The morphology of the scratch track for 2  $\mu\text{m}$   $\text{CN}_x$  film deposited on Ti-6Al-4V substrate at a normal load range between 3 and 60 N

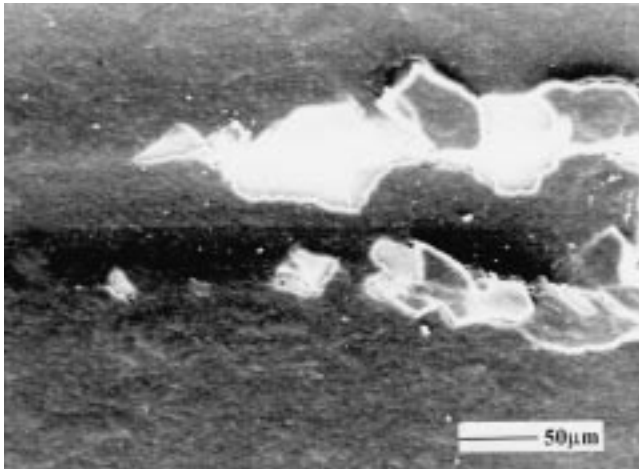


**Fig. 10** The typical morphology of the scratch track for 5  $\mu\text{m}$   $\text{CN}_x$  film deposited on plasma-nitrided Ti-6Al-4V showing the large-area spallation at a normal load range between 53 and 58 N

#### 4. Conclusions

Carbon nitride films were deposited on plasma-nitrided Ti-6Al-4V substrate in order to improve the load-bearing capacity and tribological behavior of Ti-6Al-4V. The following conclusions can be derived from the experimental results.

- Modified Vickers hardness tests showed that the intrinsic hardness of the  $\text{CN}_x$  film was about HV 2000 to 3000.

- Compared with the  $\text{CN}_x$  film deposited on Ti alloys, the load-bearing capacity of  $\text{CN}_x$  film deposited on a plasma-nitrided layer has been improved dramatically, which can be seen from both the indentation and scratch tests.
- According to the scratch tests, the duplex-treated system was effective in maintaining a favorable low and stable coefficient of friction and improving the wear resistance.

#### References

1. A.Y. Liu and M.L. Cohen: *Science*, 1989, vol. 245, p. 841.
2. M.L. Cohen: *Mater. Sci. Eng.*, 1996, vol. A209, pp. 1-4.
3. A.K. Sharma and J. Narayan: *Int. Mater. Rev.*, 1997, vol. 42, pp. 137-54.
4. P.V. Kola, D.C. Cameron, B.J. Meenan, K.A. Pischow, C.A. Anderson, N.M.D. Brown, and M.S.J. Hashmi: *Surf. Coat. Technol.*, 1995, vol. 74-75, pp. 696-703.
5. W. Ensinger: *Surf. Coat. Technol.*, 1996, vol. 84, pp. 363-75.
6. C. Niu, Y.Z. Lu, and C.M. Lieber: *Science*, 1993, vol. 261, p. 334.
7. K.M. Yu, M.L. Cohen, E.E. Haller, W.L. Hansen, A.Y. Liu, and I.C. Wu: *Phys. Rev.*, 1994, vol. B49, p. 5034.
8. J. Koskinen, J.P. Hirvonen, L. Levoska, and P. Torri: *Diamond Related Mater.*, 1996, vol. 5, p. 669.
9. A. Grill: *Surf. Coat. Technol.*, 1997, vol. 94-95, pp. 507-13.
10. Y.Q. Fu, N.L. Loh, J. Wei, B.B. Yan, and P. Hing: *Wear*, 2000, vol. 237, pp. 12-19.
11. K.T. Rie and E. Broszeit: *Surf. Coat. Technol.*, 1995, vol. 76-77, pp. 425-36.
12. Y.Q. Fu, J. Wei, N.L. Loh, B.B. Yan, and P. Hing: *J. Mater. Sci.*, 2000, vol. 35, pp. 2215-27.
13. T. Bell, H. Dong, and Y. Sun: *Tribol. Int.*, 1998, vol. 31, pp. 127-37.
14. H.H. Huang, J.L. He, and M.H. Hon: *Surf. Coat. Technol.*, 1994, vol. 64, pp. 41-46.
15. T. Michler, M. Grischke, K. Bewilogua, and A. Hieke: *Surf. Coat. Technol.*, 1999, vol. 111, pp. 41-45.
16. F.D. Lai and J.K. Wu: *Surf. Coat. Technol.*, 1996, vol. 88, pp. 183-89.
17. H. Ronkainen, J. Koskinen, S. Varjus, and K. Holmberg: *Tribol. Lett.*, 1999, vol. 6, pp. 63-73.
18. J.S. Wang, Y. Sugimura, A.G. Evans, and W.K. Tredway: *Thin Solid Films*, 1998, vol. 325, pp. 163-74.
19. J.J. Vlassak, M.D. Drory, and W.D. Nix: *J. Mater. Res.*, 1997, vol. 12, p. 1900.
20. A. Khurshudov, K. Kato, and D. Sawada: *Tribol. Lett.*, 1996, vol. 2, pp. 13-21.
21. B. Jonsson and S. Hogmark: *Thin Solid Films*, 1984, vol. 114, p. 257.
22. F. Attar: *Surf. Coat. Technol.*, 1996, vol. 78, pp. 78-86.
23. K.W. Xu: *Acta Metall. Sinica B*, 1995, vol. 31, pp. 429-34.
24. Y.Q. Fu, X.D. Zhu, K.W. Xu, and J.W. He: *J. Mater. Process. Technol.*, 1998, vol. 83, pp. 209-16.
25. K.L. Dahm, W.G. Ferguson, R. Murakami, and P.A. Dearnley: *Surf. Eng.*, 1994, vol. 10, 1994, pp. 199-204.
26. A.G. Evans and J.W. Hutchinson: *Acta Metall. Mater.*, 1995, vol. 43, p. 2507.
27. R. Wei, P.J. Wibur, and F.M. Kustas: *J. Tribol.*, 1992, vol. 114, p. 298.
28. A. Grill and V. Patel: *Diamond Related Mater.*, 1993, vol. 2, p. 1519.
29. Y. Liu, A. Erdemir, and E.I. Meletis: *Surf. Coat. Technol.*, 1996, vol. 86-87, p. 564.
30. D.M. Bailey and R.S. Sayles: *J. Tribol.*, 1991, vol. 113, pp. 133-39.